International Journal of Scientific Research & Engineering Trends
Volume 12, Issue 4, Jul-Aug-2026, ISSN (Online): 2395-566X

Combustion and Emission Characteristics of Biomass-Derived 2-Methyltetrahydrofuran Compared with 2- Methylfuran, Ethanol and Gasoline in a Direct- Injection Spark Ignition Engine

Rafiu Kayode.Olalere[1], Hongming Xu[2], Sheriff Lamidi[3], Y.O Bankole[4]
[1]Department of Mechanical Engineering, University of Birmingham, Birmingham, United Kingdom
Department of Mechanical Engineering, Lagos State University of Science and Technology, Lagos, Nigeria
[2]Department of Mechanical Engineering, University of Birmingham, Birmingham, United Kingdom
[3]Department of Mechanical Engineering, Lagos State University of Science and Technology, Lagos, Nigeria
[4]Department of Mechanical Engineering, Lagos State University of Science and Technology, Lagos, Nigeria

Abstract- The growing demand for carbon-neutral transportation has intensified research into renewable oxygenated fuels capable of improving engine efficiency while reducing exhaust emissions. Among emerging biofuels, biomass-derived 2-methyltetrahydrofuran (MTHF) has attracted considerable attention because of its favourable physicochemical properties. Nevertheless, comprehensive experimental comparisons of neat MTHF with gasoline, 2-methylfuran (MF), and ethanol under identical direct-injection spark-ignition (DISI) engine operating conditions remain limited. This study experimentally investigates the combustion characteristics, engine performance, gaseous emissions, and particulate emissions of neat MTHF relative to commercial gasoline (ULG95), MF, and ethanol using a single-cylinder DISI engine. Experiments were conducted at a constant engine speed of 1500 rpm, stoichiometric operation ($\lambda = 1$), and engine loads ranging from 3.5 to 8.5 bar indicated mean effective pressure (IMEP). Ignition timing for each fuel was optimized using the maximum brake torque (MBT) criterion or knock-limited spark advance (KLSA). At 5.5 bar IMEP, MTHF generated peak in-cylinder pressures of about 10%, 15%, and 25% higher than MF, ethanol, and gasoline, respectively. Compared with MF and ethanol, MTHF reduced indicated specific fuel consumption by approximately 8% and 33%, while maintaining thermal efficiency comparable to gasoline. Furthermore, MTHF produced lower total hydrocarbon and particulate emissions than gasoline and MF, together with lower NO_x emissions than MF. These findings demonstrate that MTHF is a promising renewable gasoline substitute capable of simultaneously enhancing combustion performance and reducing exhaust emissions in modern DISI engines.

Keywords- Include at least 4 keywords or phrases, must be separated by commas to distinguish them.

I. INTRODUCTION

Biomass-derived oxygenated fuels have attracted particular attention because the oxygen contained within their molecular structures promotes more complete combustion, improving combustion efficiency while reducing carbon monoxide, unburned hydrocarbon and particulate emissions [1]–[5]. Among commercially available oxygenated fuels, ethanol has become the most widely adopted renewable gasoline substitute owing to its high-octane rating, renewable origin and well-established production technologies. Nevertheless, ethanol presents several inherent limitations that restrict its application at high blending ratios [6]-[12]. Its relatively low heating value increases volumetric fuel consumption, while its high latent heat of vaporisation can adversely influence cold-start performance under low ambient temperatures.

Furthermore, the hygroscopic nature of ethanol creates storage, transportation and material compatibility challenges, particularly in regions with existing fuel distribution infrastructure designed for petroleum fuels [13]- [18]. These limitations have encouraged the search for alternative renewable fuels possessing physicochemical properties more closely resembling those of gasoline while maintaining the environmental benefits associated with biomass-derived oxygenated compounds. Recent developments in catalytic biomass conversion have led to the emergence of furan-based biofuels as promising next-generation gasoline substitutes. Furan compounds are primarily produced from lignocellulosic biomass through the catalytic conversion of platform molecules such as furfural and 5-hydroxymethylfurfural, thereby avoiding direct competition with food resources [19]-[26].

Compared with first-generation biofuels, these second-generation fuels generally possess higher energy densities, lower hygroscopicity and improved storage stability, making them more suitable for practical transportation applications [27]. Their molecular structures also provide favourable anti-knock characteristics, enabling efficient operation in modern downsized and turbocharged spark-ignition engines [28][29]. Among the various furan-derived fuels, 2-methylfuran (MF) has received considerable research attention because of its high-octane number, relatively high heating value and combustion properties that closely resemble those of gasoline [30] [31]. Experimental investigations have demonstrated that MF can improve combustion stability while reducing carbon monoxide emissions under suitable operating conditions. However, its aromatic furan ring contributes to increased soot precursor formation under certain combustion environments and may influence hydrocarbon speciation and particulate emissions.

Consequently, researchers have explored hydrogenated derivatives of MF in an effort to retain favourable combustion characteristics while improving oxidation behaviour. One of the most promising hydrogenated derivatives is 2-methyltetrahydrofuran (MTHF), which is produced by catalytic hydrogenation of methylfuran. The saturation of the furan ring significantly alters the physicochemical properties of the fuel, resulting in improved chemical stability, lower tendency for soot formation and combustion behaviour that is more compatible with modern direct-injection spark-ignition engines [32], [33]. Owing to its relatively high energy density, favourable volatility and renewable production pathway, MTHF has recently attracted increasing international interest as a sustainable gasoline replacement. Nevertheless, comprehensive experimental studies directly comparing MTHF with MF, ethanol and gasoline under identical DISI engine operating conditions remain limited, highlighting the need for further systematic investigations [34]-[37].

Hydrogenation of the furan ring to produce MTHF modifies the molecular structure, reduces aromaticity and changes the oxidation chemistry of the fuel. These structural differences suggest that MTHF may provide cleaner combustion while maintaining many of the desirable fuel properties exhibited by MF [38]-[43]. Nevertheless, experimental evidence directly validating these advantages under identical operating conditions remains relatively scarce. Furthermore, relatively few investigations have systematically examined the combined influence of fuel molecular structure and fuel injection strategy on combustion behaviour, engine efficiency and pollutant formation within a single experimental programme [37]-[38]. Accordingly, the present study seeks to address these knowledge gaps through a systematic experimental investigation of combustion characteristics, engine performance, regulated gaseous emissions and hydrocarbon speciation of biomass-derived MTHF compared with MF, ethanol and commercial gasoline in a direct-injection spark-ignition engine.

II. EXPERIMENTAL SECTION

The experimental investigation was conducted using a single-cylinder, four-stroke, spray-guided direct-injection spark-ignition (DISI) research engine at the engine test laboratory of the University of Birmingham. The principal specifications of the engine are summarized in Table 1, while a schematic representation of the experimental arrangement is presented in Figure 1.

Engine Setup

Prior to each experimental run, the engine was operated until thermal equilibrium was established. Independent heating and circulation systems were employed for both the engine coolant and lubricating oil to ensure stable operating conditions throughout the experiments. The coolant temperature was maintained at 85 ± 5 °C, while the lubricating oil temperature was controlled at 90 ± 3 °C. Maintaining constant thermal conditions minimized variations in combustion behaviour caused by fluctuations in engine temperature. The intake air system incorporated a 100 L surge tank to dampen intake pressure pulsations and provide a stable air supply to the engine. Fuel was delivered through a high-pressure gasoline direct injection (GDI) system operating at a constant injection pressure of 15 MPa (150 bar).

Engine speed was maintained at 1500 rpm using an eddy-current dynamometer, thereby ensuring steady-state operating conditions irrespective of variations in engine load. In-cylinder pressure was measured using a water-cooled Kistler 6041A piezoelectric pressure transducer mounted flush with the cylinder head. The pressure signal was amplified using a Kistler 5011 charge amplifier before acquisition through a National Instruments high-speed data acquisition system. Custom-developed LabVIEW software was employed for real-time data acquisition, combustion analysis, and engine control. Crank angle position was measured using a 1440-pulse crankshaft encoder, providing a resolution of 0.5 crank-angle degree (CAD).

The encoder signal served as the reference for synchronizing fuel injection, ignition timing, combustion analysis, and variable valve timing through the Engine Timing Control System (ETCS). The exhaust system incorporated an expansion chamber to attenuate exhaust pressure pulsations prior to measurement of the air-fuel ratio using a lambda sensor. Regulated gaseous emissions, including carbon monoxide (CO), unburned hydrocarbons (HC), and oxides of nitrogen (NOx), were measured using a HORIBA MEXA-700 emission analyser. Exhaust gas samples were extracted approximately 300 mm downstream of the exhaust port at a sampling flow rate of approximately 200 L min^{-1}. Particle number (PN) emissions and particle size size distributions were measured using a Cambustion DMS500 fast particulate spectrometer, which provides high-resolution particle measurements over a broad particle size range using both primary and secondary dilution systems.

This instrument enabled simultaneous determination of particle number concentration and particle size distribution under steady-state engine operating conditions. Throughout the investigation, the engine was operated at a constant speed of 1500 rpm under stoichiometric combustion conditions ($\lambda = 1$). Engine load was varied from 3.5 to 8.5 bar IMEP in increments of 1 bar. For each operating condition, ignition timing was adjusted to the Minimum Spark Advance for Best Torque (MBT). Where knock was detected, ignition timing was retarded by 2 CAD, and the resulting ignition timing was designated as the Knock-Limited Spark Advance (KLSA).

Test Fuels
The physical and chemical properties of the four fuels investigated are summarized in Table 2. Commercial RON95 unleaded gasoline (ULG95) was supplied by Shell Global Solutions (UK) and was selected as the baseline fuel owing to its widespread commercial application and high-octane rating. The renewable cyclic ether fuels, 2-

Table1: Engine Specification

Engine Type	4 Stroke ,4Valve
Combustion System	Spray guided DISI
Displacement	497cc
Bore x Stroke	83mm x 92mm
Compression Ratio	11.5:1
Fuel Type	MTHF, MF, Ethanol and Gasoline
Engine speed/ DI Pressure	1500rpm/15MPa
Intake valve open	16.5bTDC
Exhaust valve closed	36.7aTDC

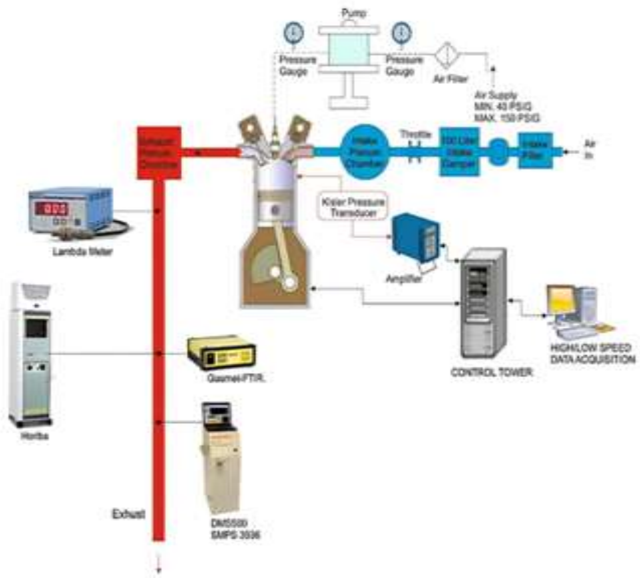

Fig.1: Engine experimental setup

methylfuran (MF) and 2- methyltetrahydrofuran (MTHF), were obtained from Fisher Scientific (UK) with a certified purity exceeding 99%. The MTHF supplied for this investigation contained 1 wt.% butylated hydroxytoluene (BHT) as a stabilizing additive to inhibit oxidative degradation during storage. Fuel-grade ethanol was obtained from the School of Biosciences, University of Birmingham. All fuel properties used in this study were obtained from manufacturer specifications and published literature and are summarized in Table 2.

Table2: Base fuel Properties [8-10;19,20]

FUEL PROPERTIES	ULG	MF	MTHF	ETH
Molecular formula	C_2-C_{14}	C_5H_6O	$C_5H_{10}O$	C_2H_60
Lower heating value MJ/Kg	42.9	31.2	34.12	26.9
Lower heating value MJ/L	31.9	27.63	28.97	21.3
Research octane number (RON)	96.8	103	88.2	107
Motor octane number	85.7	86	71.2	89
Stoichiometric air-fuel ratio	14.46	10.05	11.16	8.95
Heat of vaporisation (KJ/Kg)	373	358	375.3	840
Reid vapour Pressure (Kpa)	32.8	18.5	13.6	5.83
Density 20^0c (Kg/m3)	744.6	913.2	854	790.9
H/C ratio	1.795	1.8	1.96	3
Gravimetric O_2 content.(%)	0	19.49	18.58	34.78
Initial boiling point (^{0}c)	32.8	64	80.3	78.4
Solubility in water (vol %)	Negligible	0.3	0.01	13
Flash Point(^{0}C)	-40	1	26 (-10)	

III. RESULT AND DISCUSSION

This section presents a comprehensive comparison of the combustion characteristics, engine performance, fuel economy, regulated gaseous emissions, and particulate emissions of gasoline, 2-methylfuran (MF), 2-methyltetrahydrofuran (MTHF), and ethanol in the direct-injection spark-ignition (DISI) engine. The engine was operated at a constant speed of 1500 rpm under stoichiometric conditions ($\lambda = 1$) over an indicated mean effective pressure (IMEP) range of 3.5–8.5 bar. For each operating condition, the ignition timing was optimized to the Minimum Spark Advance for Best Torque (MBT) or adjusted to the Knock-Limited Spark Advance (KLSA) when knock occurred.

Peak In-Cylinder Pressure

Figure 3.1 illustrates the variation of peak in-cylinder pressure with engine load, represented by indicated mean effective pressure (IMEP), for gasoline (ULG), ethanol (ETH), 2-methylfuran (MF), and 2-methyltetrahydrofuran (MTHF). For all fuels, peak cylinder pressure generally increased with increasing engine load owing to the greater mass of inducted charge and the corresponding increase in heat released during combustion. Among the fuels investigated, MF consistently produced the highest peak cylinder pressure, particularly at medium and high loads, indicating faster combustion development and more effective energy release. This behaviour can be attributed to the high research octane number and favourable combustion characteristics of MF, which permit more advanced ignition timing while maintaining stable combustion. Ethanol exhibited a similar increasing trend and approached the combustion performance of MF at higher loads. [5] [39]- [43]

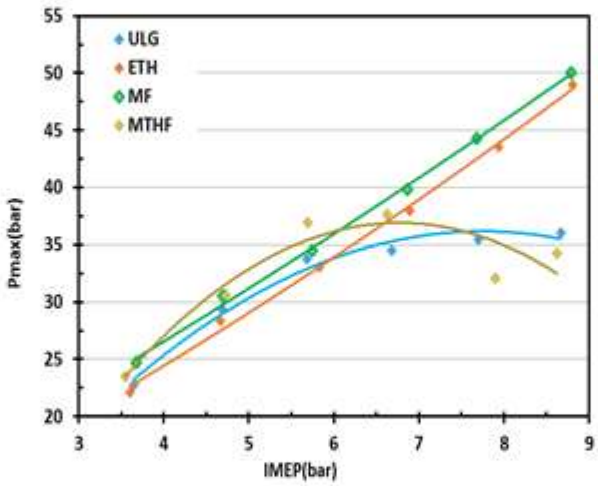

Fig. 3.1 Comparison of peak cylinder pressure as a function of IMEP for gasoline, ethanol, MF, and MTHF in a direct-injection spark-ignition engine

Spark advance

Figure 3.2 illustrates the variation of optimum spark advance with engine load for gasoline (ULG), ethanol (ETH), 2-methylfuran (MF), and 2-methyltetrahydrofuran (MTHF). For all fuels, the optimum spark advances generally decreased with increasing IMEP owing to the higher in-cylinder pressure and temperature associated with increased engine load, which accelerate combustion and increase the tendency for knock. Consequently, ignition timing was progressively retarded to achieve either the Minimum Spark Advance for Best Torque (MBT) or the Knock-Limited Spark Advance (KLSA). Among the fuels investigated, ethanol consistently required the least spark retard, maintaining spark advances of approximately 23–24°bTDC even at high loads.

This behaviour is attributed to its high research octane number and significant charge-cooling effect resulting from its large latent heat of vaporization, both of which enhance knock resistance. In contrast, gasoline and MTHF exhibited substantial spark retard at higher IMEP, indicating greater knock sensitivity under elevated load conditions. Although MTHF possesses a relatively high-octane rating compared with gasoline, its knock resistance was lower than that of ethanol under the present operating conditions. MF displayed intermediate behaviour, requiring less spark retard than gasoline while maintaining stable combustion over the entire load range. These results demonstrate that the ignition characteristics of renewable cyclic ether fuels are governed by the combined effects of octane quality, evaporation characteristics, and combustion kinetics, which directly influence combustion phasing and engine performance [5] [45] - [49].

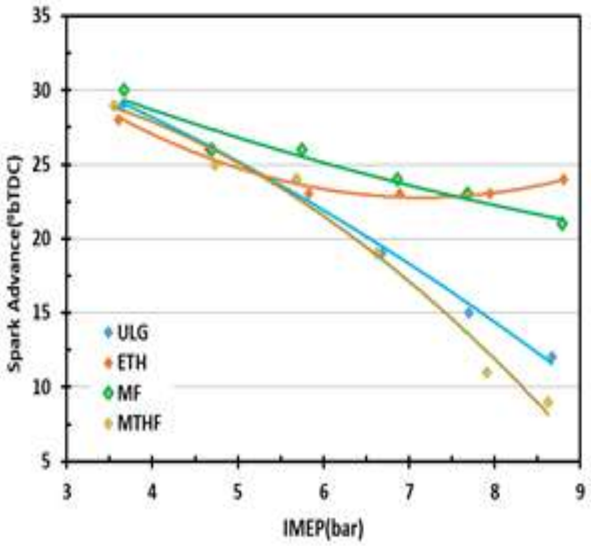

Fig. 3.2 Effect of engine load (IMEP) on optimum spark advance for gasoline, ethanol, MF, and MTHF in a direct-injection spark-ignition engine

Indicated thermal Efficiency

Figure 3.3 compares the variation of indicated thermal efficiency (ITE) with engine load for gasoline (ULG), ethanol (ETH), 2-methylfuran (MF), and 2-methyltetrahydrofuran (MTHF). In general, the indicated thermal efficiency increased with increasing IMEP for all fuels, reflecting improved utilization of the released chemical energy at higher engine loads due to reduced relative heat transfer losses and enhanced combustion efficiency. Ethanol consistently exhibited the highest indicated thermal efficiency across the investigated load range, increasing from approximately 0.324 at low load to about 0.370 at the highest IMEP. This improvement is primarily attributed to its superior knock resistance and high latent heat of vaporization, which permit more advanced ignition timing and improve volumetric efficiency through enhanced charge cooling.

MF also demonstrated higher thermal efficiency than gasoline, particularly at medium and high loads, indicating favourable combustion characteristics and efficient energy conversion. In contrast, gasoline and MTHF showed comparatively lower efficiencies, with only marginal improvements as engine load increased. For MTHF, the relatively lower efficiency at high loads is consistent with the increased spark retard required under knock-limited operating conditions, which delays combustion phasing and reduces the fraction of heat released near top dead centre. Overall, the results indicate that renewable oxygenated fuels, particularly ethanol and MF, provide improved thermal efficiency compared with conventional gasoline under the investigated DISI engine operating conditions, highlighting their potential for enhancing engine performance while supporting sustainable transportation [5] [45].

Indicated thermal Efficiency

Figure 3.3 compares the variation of indicated thermal efficiency (ITE) with engine load for gasoline (ULG), ethanol (ETH), 2-methylfuran (MF), and 2-methyltetrahydrofuran (MTHF). In general, the indicated thermal efficiency increased with increasing IMEP for all fuels, reflecting improved utilization of the released chemical energy at higher engine loads due to reduced relative heat transfer losses and enhanced combustion efficiency.

Ethanol consistently exhibited the highest indicated thermal efficiency across the investigated load range, increasing from approximately 0.324 at low load to about 0.370 at the highest IMEP. This improvement is primarily attributed to its superior knock resistance and high latent heat of vaporization, which permit more advanced ignition timing and improve volumetric efficiency through enhanced charge cooling.

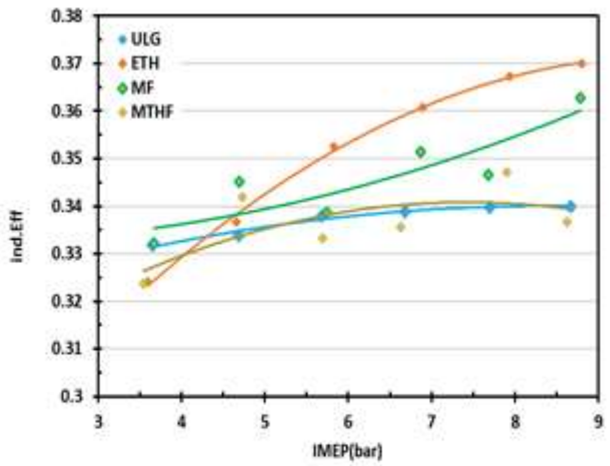

Fig. 3.3. Effect of engine load (IMEP) on indicated thermal efficiency for gasoline, ethanol, MF, and MTHF in a direct-injection spark-ignition engine

MF also demonstrated higher thermal efficiency than gasoline, particularly at medium and high loads, indicating favourable combustion characteristics and efficient energy conversion. In contrast, gasoline and MTHF showed comparatively lower efficiencies, with only marginal improvements as engine load increased. For MTHF, the relatively lower efficiency at high loads is consistent with the increased spark retard required under knock-limited operating conditions, which delays combustion phasing and reduces the fraction of heat released near top dead centre. Overall, the results indicate that renewable oxygenated fuels, particularly ethanol and MF, provide improved thermal efficiency compared with conventional gasoline under the investigated DISI engine operating conditions, highlighting their potential for enhancing engine performance while supporting sustainable transportation [5] [45].

Indicated Specific Fuel Consumption

Figure 3.4 presents the variation of indicated specific fuel consumption (ISFC) with work as engine load increased. At higher loads, the proportion of heat losses and pumping losses relative to the total energy released decreases, leading to improved engine efficiency and consequently lower fuel consumption. Gasoline consistently exhibited the lowest ISFC throughout the investigated load range, primarily because of its high lower heating value (LHV), which requires less fuel mass to produce a given engine output. Ethanol showed the highest ISFC, decreasing from approximately 415 g kWh^{-1} at low load to about 365 g kWh^{-1} at high load.

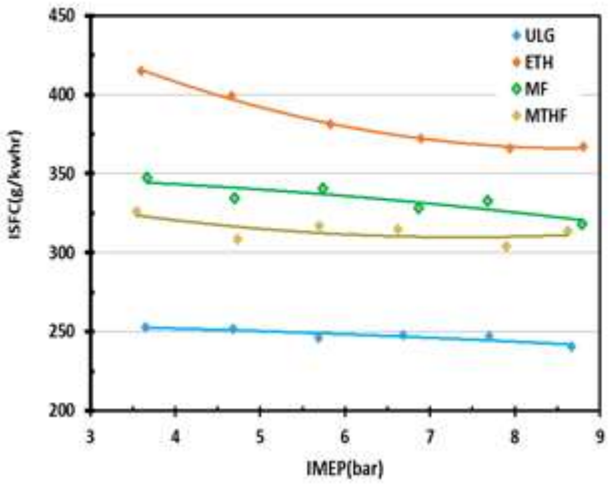

Fig.3.4. Comparison of indicated specific fuel consumption as a function of IMEP for gasoline, ethanol, MF, and MTHF under stoichiometric combustion

This behaviour is attributed to its significantly lower heating value compared with gasoline, requiring a greater mass of fuel to achieve equivalent power output despite its superior combustion efficiency. MF exhibited intermediate fuel consumption characteristics, while MTHF consistently recorded lower ISFC than MF but higher values than gasoline. The relatively lower ISFC of MTHF compared with MF can be attributed to its higher volumetric energy density and favourable combustion characteristics, which improve energy utilization. These results indicate that although renewable oxygenated fuels generally require higher fuel consumption than gasoline because of their lower energy content, MTHF offers a favourable compromise between combustion performance and fuel economy, making it a promising renewable gasoline substitute for direct-injection spark-ignition engines [5][35]. Engine load for gasoline (ULG), ethanol (ETH), 2-methylfuran (MF), and 2-methyltetrahydrofuran (MTHF). For all fuels, ISFC generally decreased with increasing IMEP, reflecting the improved conversion of fuel chemical energy l[5].

Combustion Phasing (CA50)

Figure 3.5 presents the variation of combustion phasing, expressed as the crank angle corresponding to 50% mass fraction burned (CA50), with engine load for gasoline (ULG),

International Journal of Scientific Research & Engineering Trends
Volume 12, Issue 4, Jul-Aug-2026, ISSN (Online): 2395-566X

ethanol (ETH), 2-methylfuran (MF), and 2-methyltetrahydrofuran (MTHF). At low engine loads, all four fuels exhibited similar combustion phasing, with CA50 occurring between approximately 8 and 9 CAD, indicating comparable combustion development under relatively mild operating conditions. As engine load increased, gasoline and MTHF showed a pronounced shift of CA50 towards later crank angles, whereas ethanol and MF maintained nearly constant combustion phasing throughout the investigated load range.

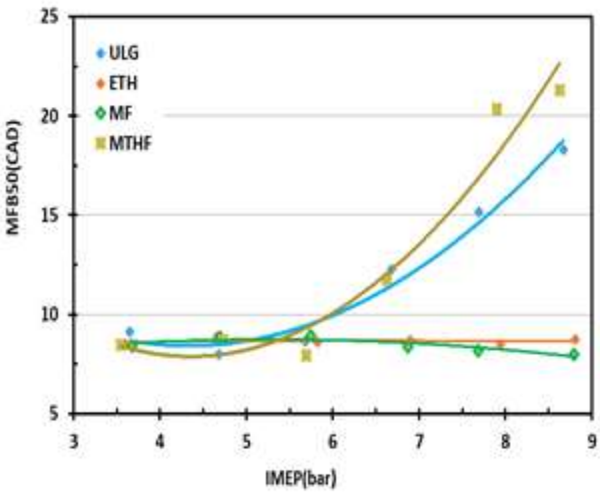

Fig.3.5. Influence of engine load on combustion phasing (CA50) for gasoline and renewable cyclic ether fuels (MF and MTHF), with ethanol as a benchmark oxygenated fuel.

The delayed combustion observed for gasoline and particularly MTHF is primarily attributed to the increased ignition retard imposed by knock-limited spark advance (KLSA) at higher loads, which delays the main heat-release process. In contrast, the superior knock resistance of ethanol and MF permitted more advanced ignition timing, thereby maintaining combustion phasing close to the optimum location for efficient energy conversion. Since combustion phasing strongly influences thermal efficiency, pressure development and fuel economy, maintaining CA50 near the optimum crank angle is essential for maximizing engine performance. The stable combustion phasing achieved with ethanol and MF is consistent with their higher indicated thermal efficiencies [5] [31].

Combustion Durations (CAD50- CAD90)

Figure 3.6 illustrates the variation of combustion duration (CA10–CA90) with indicated mean effective pressure (IMEP) for ULG, ETH, MF, and MTHF) . Combustion duration represents the crank-angle interval required for the cumulative heat release to increase from 10% to 90% of the total released energy and is an important indicator of combustion efficiency and flame propagation. At low engine loads, all four fuels exhibited comparable combustion durations of approximately 20–22 CAD. As engine load increased, MF maintained the shortest and most stable combustion duration throughout the investigated operating range, indicating rapid flame development and efficient combustion. Ethanol also exhibited relatively stable combustion duration, reflecting its high flame speed and excellent knock resistance. In contrast, gasoline and MTHF showed progressively longer combustion durations at higher IMEP, with MTHF displaying the greatest increase under high-load conditions. This behaviour is consistent with the increased ignition retard required under knock-limited operating conditions, which delays combustion phasing and prolongs the main heat-release process. Longer combustion duration shifts a greater proportion of heat release away from top dead centre, thereby reducing the effectiveness of pressure development and thermal efficiency.

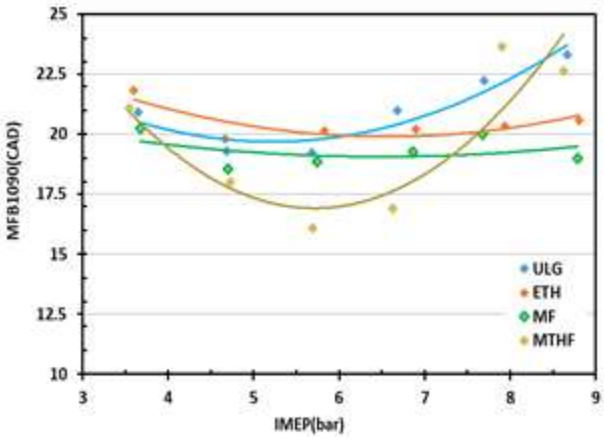

Fig.3.6. Effect of engine load on combustion duration (CA10–CA90) for gasoline, ethanol, MF, and MTHF in a direct-injection spark-ignition engine

The shorter combustion duration observed for MF contributes to its superior combustion performance and complements the higher peak cylinder pressure and indicated thermal efficiency reported in the preceding sections. [5]

Gaseous Emissions (Nox, CO and HC Emissions)

The gaseous emission characteristics of gasoline (ULG), ethanol (ETH), 2-methylfuran (MF), and 2-

International Journal of Scientific Research & Engineering Trends
Volume 12, Issue 4, Jul-Aug-2026, ISSN (Online): 2395-566X

methyltetrahydrofuran (MTHF) were evaluated under stoichiometric operating conditions over the investigated engine load range. The analysis focused on the regulated emissions of carbon monoxide (CO), unburned hydrocarbons (HC), and oxides of nitrogen (NO_x), which are widely used to assess combustion efficiency and environmental performance. Differences in the molecular structure, oxygen content, volatility, and combustion characteristics of the fuels significantly influence the formation of these pollutants. Oxygenated fuels generally promote more complete oxidation of the fuel–air mixture, leading to lower CO and HC emissions, although the resulting increase in combustion temperature may affect NO_x formation. The measured gaseous emissions are therefore discussed in relation to the combustion characteristics presented in the preceding sections, particularly combustion phasing, combustion duration, and indicated thermal efficiency [5][37].

This integrated analysis provides a comprehensive understanding of the emission behaviour of renewable cyclic ether fuels relative to conventional gasoline and ethanol in a direct-injection spark-ignition engine [41]. Figures 3.7(a–c) present the variations of indicated carbon monoxide (ISCO), indicated unburned hydrocarbon (ISHC), and indicated nitrogen oxides ($ISNO_x$) emissions with engine load for gasoline (ULG), ethanol (ETH), 2-methylfuran (MF), and 2-methyltetrahydrofuran (MTHF). In general, both CO and HC emissions decreased with increasing IMEP for all fuels, indicating improved combustion efficiency at higher loads due to enhanced flame propagation and more complete oxidation of the fuel-air mixture. Ethanol consistently produced the lowest CO and HC emissions throughout the load range, which can be attributed to its high oxygen content that promotes more complete combustion.

MTHF also exhibited lower CO and HC emissions than gasoline and MF, particularly at medium and high loads, demonstrating the beneficial effect of oxygenated cyclic ether fuels on reducing incomplete combustion products. Gasoline produced the highest CO and HC emissions owing to the absence of chemically bound oxygen and comparatively poorer mixture oxidation. Conversely, NO_x emissions generally increased with engine load for all fuels because of the higher in-cylinder temperatures associated with increased combustion intensity. MF and MTHF exhibited slightly higher NO_x emissions than gasoline over most operating conditions, reflecting their improved combustion characteristics and higher local flame temperatures. Ethanol showed the lowest NO_x emissions at low engine loads but approached the emission levels of

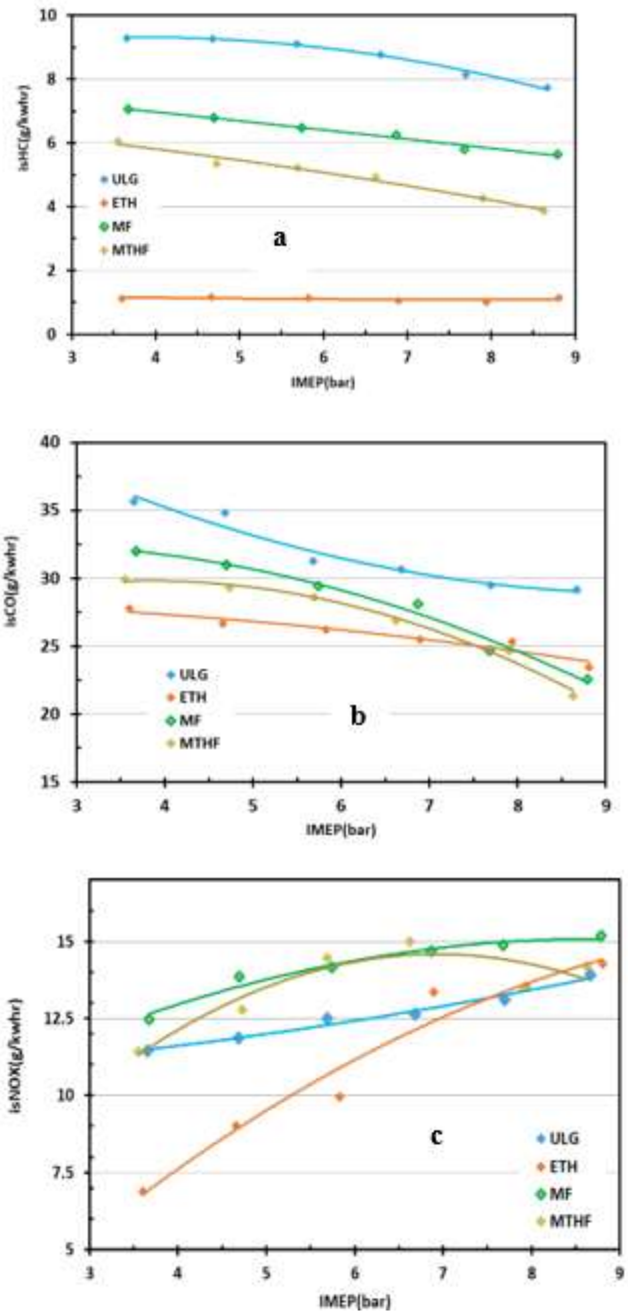

Fig. 3.7(a) Variation of ISCO with indicated mean effective pressure (IMEP) for ULG, ETH, MF, and MTHF. (b). Variation of ISHC with indicated mean effective pressure (IMEP) for ULG, ETH, MF, and MTHF (c). Variation $ISNO_x$ with indicated mean effective pressure (IMEP) for ULG), ETH, MF, and MTHF gasoline at higher loads. The combined results

indicate that renewable oxygenated fuels significantly reduce incomplete combustion products (CO and HC) while slightly increasing NO_x formation because of more efficient combustion. Overall, MTHF demonstrated a favourable balance between combustion efficiency and regulated gaseous emissions, supporting its potential as a sustainable gasoline substitute in direct-injection spark-ignition engines. [36]

Particulate Emissions

Figure 3.8(a–c) compares the particle number size distributions of gasoline (ULG), ethanol (ETH), 2-methylfuran (MF), and 2-methyltetrahydrofuran (MTHF) at three representative engine loads under stoichiometric operating conditions. The distributions were measured using a Cambustion DMS500 fast particle spectrometer and provide insight into the influence of fuel molecular structure on particle formation in a direct-injection spark-ignition engine [5][41]. In all operating conditions, the particle size distributions were dominated by the nucleation mode, with the highest particle concentrations occurring within the diameter range of approximately 8–20 nm.

This behaviour is characteristic of gasoline direct-injection engines, where rapid cooling and dilution of exhaust gases promote the formation of ultrafine particles immediately after combustion. At all engine loads, gasoline consistently produced the highest particle number concentration throughout the measured particle size range. The peak particle concentration occurred near 10–15 nm, indicating significant nucleation of soot precursors formed within locally fuel-rich regions during spray impingement and incomplete fuel evaporation. Since gasoline contains no chemically bound oxygen, oxidation of intermediate hydrocarbon species is less effective, resulting in greater formation of soot nuclei and condensed hydrocarbon particles. Similar observations have been reported for gasoline direct-injection engines operating under stoichiometric conditions, where wall wetting and heterogeneous mixture formation are recognised as major contributors to particulate emissions [47].

In contrast, ethanol consistently generated the lowest particle number concentrations across the entire particle diameter range at all operating conditions. The substantial reduction in particle emissions can be attributed to its high oxygen content (approximately 35 wt.%), high latent heat of vaporization and absence of aromatic compounds. The chemically bound oxygen promotes oxidation of soot precursors during combustion, while the cooling effect associated with fuel evaporation improves charge homogeneity and suppresses locally fuel-rich regions where soot formation is initiated. Consequently, ethanol exhibited the smallest nucleation-mode peak among all fuels investigated. MF and MTHF produced intermediate particle emissions between gasoline and ethanol. Although both fuels are oxygenated and biomass-derived, their particle formation characteristics differed slightly because of differences in molecular structure and physicochemical properties.

MF generally produced higher particle concentrations than MTHF, particularly near the peak nucleation-mode diameter. This behaviour is likely associated with the unsaturated furan ring structure of MF, which can facilitate the formation of aromatic intermediates and soot precursors during high-temperature oxidation. By comparison, MTHF possesses a saturated cyclic ether structure that is less prone to aromatic growth reactions, thereby suppressing soot precursor formation and reducing particle number emissions.

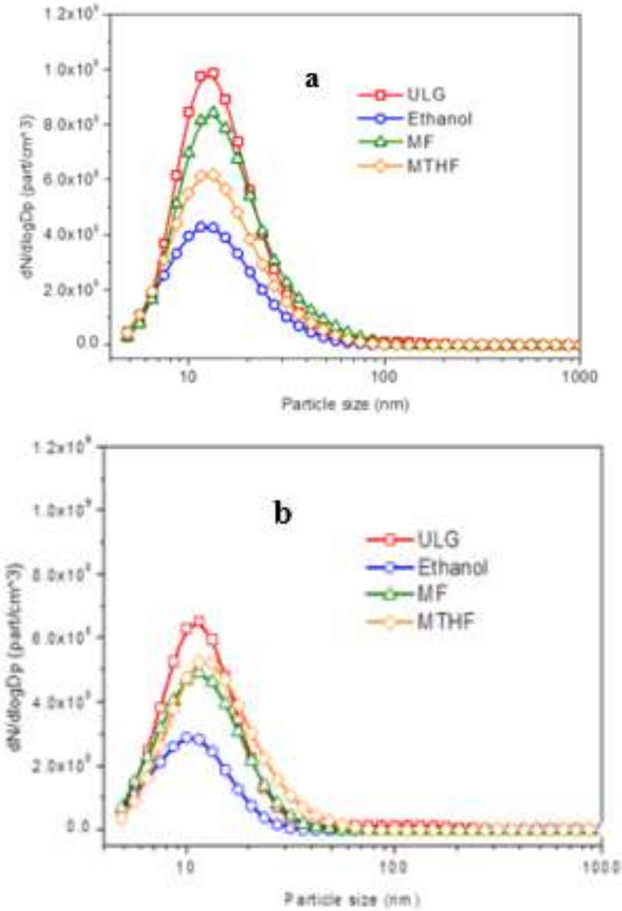

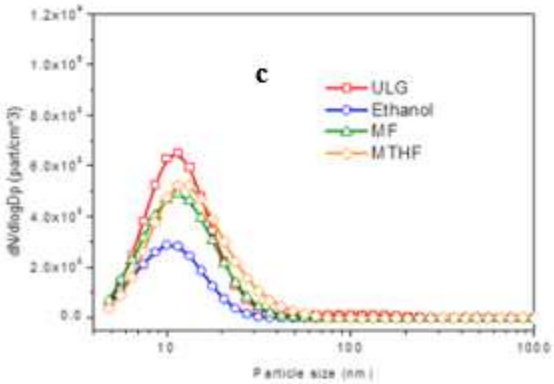

Fig.3.8 Particle number size distributions of gasoline (ULG), ethanol, (ET 2-methylfuran (MF), and 2-mMethyltetrahydrofuran (MTHF) under stoichiometric operation at (a) low load, (b) medium load, and (c) high load

particles. The overall particle distributions therefore reflect the balance between particle generation and oxidation under each operating condition. Despite these load-dependent changes, the relative ranking of the fuels remained largely unchanged, with gasoline producing the highest particle emissions, followed by MF, MTHF and ethanol. MTHF, although requiring greater spark retard at high loads because of knock-limited operation, still produced considerably fewer particles than gasoline owing to its oxygenated molecular structure and improved mixture preparation. These findings demonstrate that renewable cyclic ether fuels can significantly reduce particulate emissions from DISI engines while maintaining competitive combustion performance. In particular, MTHF offers a favourable compromise between combustion efficiency, fuel economy and particulate emission reduction, supporting its potential as a sustainable alternative to conventional gasoline in future spark-ignition engine

IV. CONCLUSION

Based on the experimental investigation of gasoline (ULG), ethanol (ETH), 2-methylfuran (MF), and 2-methyltetrahydrofuran (MTHF) in a direct-injection spark-ignition engine, the following conclusions are drawn:

- MF exhibited the most favourable combustion characteristics, producing the highest peak cylinder pressure (approximately 40% higher than gasoline at maximum load) and maintaining advanced combustion phasing. The overall combustion performance ranked MF > Ethanol > MTHF > Gasoline, confirming the superior combustion reactivity of renewable cyclic ether fuels.
- Ethanol achieved the highest indicated thermal efficiency (≈9% improvement over gasoline), followed by MF (≈6%), MTHF (≈1–2%), and gasoline. Conversely, gasoline recorded the lowest indicated specific fuel consumption because of its higher heating value, whereas MTHF consumed approximately 12–15% less fuel than MF, demonstrating the benefit of its higher volumetric energy density.
- Ethanol produced the lowest CO and HC emissions, followed by MTHF, MF, and gasoline. Compared with gasoline, MTHF reduced CO and HC emissions by approximately 20–30%, while MF achieved reductions of approximately 10–20%. Improved combustion efficiency of the oxygenated fuels resulted in a moderate increase in NO_x emissions, particularly for MF.
- All fuels generated predominantly nucleation-mode particles (approximately 8–20 nm), with gasoline producing the highest particle number concentration. The particulate emission performance ranked Ethanol > MTHF > MF > Gasoline, with MTHF reducing peak particle number concentration by approximately 25–35% relative to gasoline while maintaining favourable combustion performance. This demonstrates that MTHF offers the most balanced compromise between engine performance, combustion stability, fuel economy, and emission reduction among the renewable cyclic ether fuels investigated.

V. RECOMMENDATION

Future studies should optimize engine operating parameters, including ignition timing, injection strategy, and EGR, to maximize the combustion and emission benefits of MF and MTHF. This will improve engine efficiency and knock resistance.

Advanced diagnostic techniques should be employed to investigate soot formation mechanisms and particulate characteristics of renewable cyclic ether fuels. This will enhance understanding of their combustion chemistry and emission behaviour.

Long-term durability tests, transient engine operation, and life-cycle assessments are recommended to evaluate the commercial feasibility of MF and MTHF. These studies will support their large-scale adoption as sustainable gasoline alternatives.

Symbol / Abbreviation	Definition
ATDC	After Top Dead Centre
BDC	Bottom Dead Centre
BTE	Brake Thermal Efficiency
CA	Crank Angle
CO	Carbon Monoxide
CO_2	Carbon Dioxide
DISI	Direct-Injection Spark-Ignition
GHG	Greenhouse Gas
HC	Unburned Hydrocarbons
HRR	Heat Release Rate
ICE	Internal Combustion Engine
IMEP	Indicated Mean Effective Pressure
MF	2-Methylfuran
MTHF	2-Methyltetrahydrofuran
NO_x	Nitrogen Oxides
RON	Research Octane Number
SI	Spark-Ignition
TDC	Top Dead Centre

Acknowledgements
The authors would like to thank Jaguar Motors UK, for supplying the DISI engine use for this study, as well as the University of Birmingham Uk, for the opportunity to use the engine test cells in the future engine laboratory to conduct this research study. Special appreciation to Lagos State University of Science and Technology Nigeria and Tetfund Nigeria for the scholarship funding during the research period

REFERENCES

1. International Energy Agency (IEA), CO_2 Emissions in 2024: Analysis. Paris, France: IEA Publications, 2025.
2. International Energy Agency (IEA), World Energy Outlook 2024. Paris, France: IEA Publications, 2024.
3. Intergovernmental Panel on Climate Change (IPCC), Climate Change 2022: Mitigation of Climate Change. Contribution of Working Group III to the Sixth Assessment Report of the Intergovernmental Panel on Climate Change. Cambridge, U.K.: Cambridge University Press, 2022.
4. United Nations Framework Convention on Climate Change (UNFCCC), The Paris Agreement. Bonn, Germany: United Nations, 2015.
5. J. B. Heywood, Internal Combustion Engine Fundamentals, 2nd ed. New York, NY, USA: McGraw-Hill Education, 2018.
6. S. R. Turns, An Introduction to Combustion: Concepts and Applications, 4th ed. New York, NY, USA: McGraw-Hill Education, 2021.
7. International Energy Agency (IEA), Renewables 2024: Analysis and Forecast to 2030. Paris, France: IEA Publications, 2024.
8. Organisation for Economic Co-operation and Development/International Energy Agency (OECD/IEA), Technology Roadmap: Biofuels for Transport. Paris, France: OECD Publishing, 2011.
9. T. Le, H. Nguyen, A. T. Hoang, and V. V. Pham, "Methyltetrahydrofuran and 2,5-dimethyltetrahydrofuran: A review of heterogeneous catalytic approaches," RSC Advances, vol. 15, pp. 26537–26551, 2025
10. G. Kalghatgi, Fuel/Engine Interactions. Warrendale, PA, USA: SAE International, 2018.
11. S. M. Sarathy, A. Farooq, G. T. Kalghatgi, "Recent progress in the combustion chemistry of oxygenated transportation fuels," Progress in Energy and Combustion Science, vol. 65, pp. 67–108, 2018.
12. D. M. Alonso, J. Q. Bond, and J. A. Dumesic, "Catalytic conversion of biomass to biofuels," Green Chemistry, vol. 19, no. 24, pp. 582–593, 2017.
13. M. J. Climent, A. Corma, and S. Iborra, "Conversion of biomass platform molecules into transportation fuels," Green Chemistry, vol. 16, no. 2, pp. 516–547, 2014.
14. J. C. Serrano-Ruiz, R. Luque, and A. Sepúlveda-Escribano, "Transformations of biomass-derived platform molecules into high-value chemicals and fuels," Chemical Society Reviews, vol. 40, no. 11, pp. 5266–5281, 2011.
15. C. Wang et al., "Combustion characteristics and emissions of 2-methylfuran compared with 2,5-dimethylfuran, gasoline and ethanol in a DISI engine," Fuel, vol. 103, pp. 200–211, 2013, doi: 10.1016/j.fuel.2012.05.043.
16. H. Wei et al., "Experimental investigation on the combustion and emissions characteristics of 2-methylfuran gasoline blend fuel in a spark-ignition engine," Applied Energy, vol. 132, pp. 317–324, 2014, doi: 10.1016/j.apenergy.2014.07.009.
17. M. Mohamed et al., "Impact of RON on a heavily downsized boosted SI engine using 2nd generation

biofuel—A comprehensive experimental analysis," Energy Conversion and Management: X, vol. 22, Art. no. 100557, 2024.
18. S. Coşman, "Experimental research of the effects of benzoylthiourea derivative fuel and gasoline mixtures on engine performance and emissions," Int. J. Automotive Sci. Technol., vol. 7, no. 4, pp. 403–409, 2023.
19. M. Lapuerta, O. Armas, and J. Rodríguez-Fernández, "Effect of biodiesel fuels on diesel engine emissions," Progress in Energy and Combustion Science, vol. 34, no. 2, pp. 198–223, 2008.
20. G. Kalghatgi, "Fuel anti-knock quality—Part I. Engine studies," SAE International Journal of Engines, vol. 7, no. 1, pp. 1–18, 2014.
21. A. Demirbas, Biofuels: Securing the Planet's Future Energy Needs. London, U.K.: Springer, 2009.
22. M. Balat and H. Balat, "Recent trends in global production and utilization of bioethanol fuel," Applied Energy, vol. 86, no. 11, pp. 2273–2282, 2009.
23. J. Q. Bond, D. M. Alonso, D. Wang, R. M. West, and J. A. Dumesic, "Integrated catalytic conversion of biomass to transportation fuels," Science, vol. 327, no. 5969, pp. 1110–1114, 2010.
24. J. C. Serrano-Ruiz and J. A. Dumesic, "Catalytic routes for the conversion of biomass into liquid hydrocarbon transportation fuels," Energy & Environmental Science, vol. 4, no. 1, pp. 83–99, 2011.
25. Y. Roman-Leshkov, C. J. Barrett, Z. Y. Liu, and J. A. Dumesic, "Production of dimethylfuran for liquid fuels from biomass-derived carbohydrates," Nature, vol. 447, pp. 982–985, 2007.
26. S. M. Sarathy, "Gasoline surrogate fuels and oxygenated biofuels," Progress in Energy and Combustion Science, vol. 44, pp. 40–102, 2014.
27. Thewes et al., "Analysis of the impact of 2-methylfuran on mixture formation and combustion in a direct-injection spark-ignition engine," Energy & Fuels, vol. 25, no. 12, pp. 5549–5561, 2011, doi: 10.1021/ef201021a
28. R. Daniel, H. Xu, A. P. Jones, et al., "Combustion performance of 2-methylfuran in a DISI engine," Fuel, vol. 99, pp. 72–82, 2012.
29. R. K. Olalere, Combustion Performance and Emissions Characteristics of 2-Methyltetrahydrofuran and Cyclopentanone in a DISI Engine. Ph.D. dissertation, University of Birmingham, Birmingham, U.K., 2025.
30. Abraham, J., F. V. Bracco, and R. D. Reitz. "Comparisons of computed and measured premixed charge engine combustion." Combustion and flame 60.3 (1985): 309-322.
31. Anselmi, Patricia, et al. "Renewable fuel and blend properties for the reduction of GHG emissions under different spark-ignited engine architectures." Fuel 353 (2023): 129194.
32. H. Liu, R. K. Olalere, C. Wang, X. Ma, and H. Xu, "Combustion characteristics and engine performance of 2-methylfuran compared with gasoline and ethanol in a direct-injection spark-ignition engine," Fuel, vol. 299, Art. no. 120825, 2021, doi: 10.1016/j.fuel.2021.120825.
33. R. K. Olalere et al., "Experimental study of combustion and emissions characteristics of low blend ratio of 2-methylfuran/2-methyltetrahydrofuran with gasoline in a DISI engine," Fuel, vol. 382, Art. no. 133799, 2025, doi: 10.1016/j.fuel.2024.133799
34. Zhao, Hua. "Overview of gasoline direct injection engines." Advanced direct injection combustion engine technologies and development. Woodhead Publishing, 2010. 1-19.
35. R. K. Olalere, G. Zhang, and H. Xu, "Experimental investigation of gaseous emissions and hydrocarbon speciation for MF and MTHF gasoline blends in DISI engine," International Journal of Automotive Manufacturing and Materials, vol. 3, no. 1, p. 6, 2024.
36. M. Costa and L. Sodré, "Compression ratio effects on combustion and emissions of oxygenated fuels in SI engines: A review," Renewable and Sustainable Energy Reviews, vol. 44, pp. 838–854, 2015.
37. S. K. Aggarwal, "A review of spray and combustion characteristics of alternative liquid fuels," Progress in Energy and Combustion Science, vol. 45, pp. 1–37, 2014.
38. Hoang, Anh Tuan. "2-Methylfuran (MF) as a potential biofuel: A thorough review on the production pathway from biomass, combustion progress, and application in engines." Renewable and Sustainable Energy Reviews 148 (2021): 111265.
39. R. Stone, Introduction to Internal Combustion Engines, 5th ed. London, U.K.: Palgrave Macmillan, 2021.
40. R. Daniel, H. Xu, and A. P. Jones, "Combustion characteristics of 2-methylfuran in a direct-injection spark-ignition engine," Fuel, vol. 99, pp. 72–82, 2012.
41. Le, Ngan Nguyen, et al. "One-pot production of bio-based 2-methyltetrahydrofuran and 2, 5-dimethyltetrahydrofuran: a review of heterogeneous catalytic approaches." RSC advances 15.32 (2025): 26537-26551.

42. J. B. Heywood, Internal Combustion Engine Fundamentals, 2nd ed. New York, NY, USA: McGraw-Hill Education, 2018.
43. A. C. Lewis, N. Carslaw, and P. Monks, "Volatile organic compounds and atmospheric chemistry," Atmospheric Environment, vol. 166, pp. 497–507, 2017.
44. Wang, Chongming, et al. "Combustion characteristics and emissions of 2-methylfuran compared to 2, 5-dimethylfuran, gasoline and ethanol in a DISI engine." Fuel 103 (2013): 200-211.
45. S. M. Sarathy, "Fuel molecular structure and combustion characteristics of oxygenated fuels," Progress in Energy and Combustion Science, vol. 65, pp. 67–108, 2018.